ACS Macro Letters

Letter

pubs.acs.org/macroletters

Molecular Weight Dependence of Zero-Shear Viscosity in Atactic Polypropylene Bottlebrush Polymers

Samuel J. Dalsin,[†] Marc A. Hillmyer,*[,‡] and Frank S. Bates*[,†]

[†]Department of Chemical Engineering and Materials Science and [‡]Department of Chemistry, University of Minnesota, Minneapolis, Minnesota 55455-0431, United States

Supporting Information

ABSTRACT: A series of bottlebrush polymers with atactic polypropylene side chains were synthesized via ring-opening metathesis polymerization using Grubbs' third-generation catalyst $(H_2IMes)(3\text{-}BrPy)_2(Cl)_2Ru{=}CHPh$. Polymers were prepared with fixed side chain length and variable backbone degree of polymerization (DP) ranging from 11 to 732 (M_w = 22−1500 kg/mol) and include the largest reported polyolefin-based bottlebrush polymers. The zero-shear viscosity of each polymer sample was measured using small-amplitude oscillatory shear measurements. Power law fits of zero-shear viscosity (η_0) versus weight-average molar mass ($\eta_0 \sim M_w^{\alpha}$) revealed distinct regimes with differing molecular weight dependences. A weak dependence ($\alpha < 0.5$) was observed at low molecular weight due to the increasingly compact nature of short bottlebrush polymers with the continued addition of side chains. The scaling transitioned to Rouse-like dynamics (α = 1.2) at high molecular weight as a consequence of a sphere-to-cylinder conformational change with increasing DP of the bottlebrush backbone.

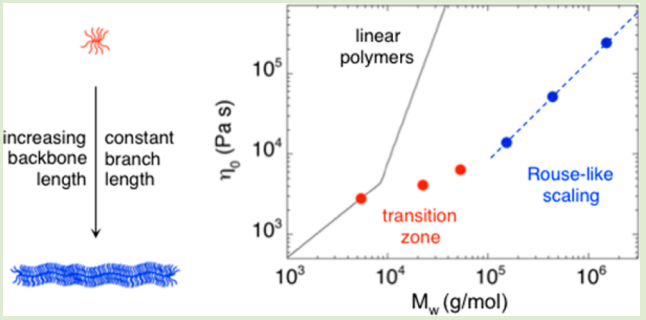

Bottlebrush polymers have gained considerable academic interest in recent years due to their extraordinary molecular architecture and unique properties.[1−3] The term "bottlebrush" generally refers to a highly branched polymer molecule composed of tightly spaced side chains arranged with regular frequency along a polymer backbone. Bottlebrushes are characterized by a persistent, cylindrical conformation resulting from excluded volume effects concomitant with a high branching density.[4−6] In the bulk, the extended conformation typically precludes the development of intermolecular entanglements and results in materials with Rouse-like relaxation dynamics (i.e., no rubbery plateau), even at molar masses exceeding 10^6 g/mol.[7−13] As a result of these unique properties, applications including rheological modifiers,[14] nanoporous materials,[15] supersoft elastomers,[10] and photonic bandgap materials[16−18] have been explored. Further development of polyolefin-based bottlebrush polymers may be especially advantageous as a means to expand the breadth of properties available to commercially viable polyolefin blends and composite materials. To this end, we have investigated the synthesis and rheological behavior of polypropylene-based bottlebrush polymers.

The bottlebrushes synthesized in this study were prepared using a grafting-through technique, which involves the polymerization of preformed monotelechelic polymers or "macromonomers". As opposed to grafting-from or grafting-onto polymerization methods, which often suffer from incomplete grafting efficiency, direct polymerization of macromonomers guarantees that one side chain is positioned on every repeat unit along the backbone. Previous investigations targeting bottlebrushes with polyolefin side chains have also employed this synthetic strategy. Reports from Rose et al.[19] and Kaneko et al.[20] have demonstrated polymerization of end-functionalized poly(ethylene-*co*-propylene) macromonomers. However, limited degrees of polymerization were observed in both cases, resulting in bottlebrush polymers with a maximum of 16 and 35 branches per molecule, respectively. More recently, Anderson-Wile et al. reported the ring-opening metathesis polymerization (ROMP) of norbornenyl-terminated syndiotactic polypropylene macromonomers to produce bottlebrushes with up to 50 branches per molecule on average.[21] They highlighted the utility of ROMP, which has become an attractive route toward bottlebrush polymers due to the development of highly active ruthenium-based metathesis catalysts.[22,23] Moreover, the fast-initiating third-generation Grubbs' catalyst ($(H_2IMes)(3\text{-}BrPy)_2(Cl)_2Ru{=}CHPh$; **G3**) has proven to be remarkably effective in promoting the living ROMP of norbornenyl-functionalized macromonomers.[11,24,25]

In this Letter, we report the synthesis and ROMP of norbornenyl-terminated atactic polypropylene (aPP) macromonomers using **G3** to produce bottlebrush polyolefins with degrees of polymerization over an order of magnitude greater than previously reported. The complex viscosity (η^*) of each

Received: February 8, 2014
Accepted: April 10, 2014
Published: April 15, 2014

   dx.doi.org/10.1021/mz500082h | *ACS Macro Lett.* 2014, 3, 423−427

sample was measured using small-amplitude oscillatory shear measurements, and the zero-shear viscosity (η_0) was determined as the limiting complex viscosity at decreasing frequency, $\eta_0 = \lim(\eta^*)_{\omega\to 0}$. The results reveal two regimes with disparate scaling of η_o with weight-average molar mass (M_w).

Bottlebrush polymers were synthesized following the procedure presented in Scheme 1. Initially, a vinyl-terminated

Scheme 1. Synthesis and Polymerization of aPP-NB Macromonomers

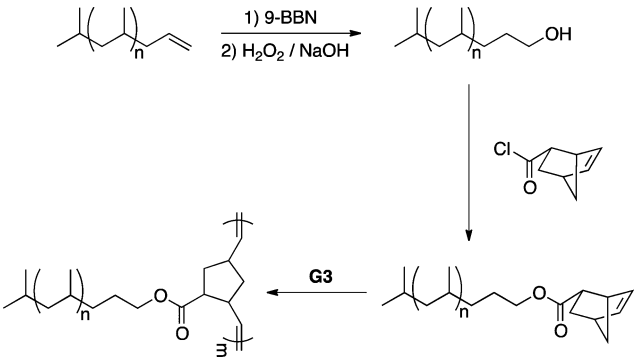

aPP starting material (M_n = 1.75 kg/mol; $Đ$ = 1.65) provided by ExxonMobil Chemical Co. was converted to hydroxyl-terminated aPP (aPP-OH) using a two-step hydroboration–oxidation reaction. 9-Borabicyclo[3.3.1]nonane (9-BBN) was chosen as the hydroboration agent and is known to undergo highly regioselective anti-Markovnikov addition to alkenes.[26] Thus, aPP-OH was exclusively produced with primary alcohol end-groups following oxidation with hydrogen peroxide. Conversion of the vinyl terminus was indicated by the elimination of alkene resonances in the ^{1}H NMR spectrum (Figure S2, Supporting Information). Purified aPP-OH molecules were subsequently transformed to norbornenyl-terminated aPP (aPP-NB) by coupling with *exo*-5-norbornene-2-carbonyl chloride. The pure *exo* isomer was utilized in this reaction as *exo*-substituted norbornene derivatives have been shown to participate in ROMP with Grubbs' catalysts much more readily than *endo*/*exo* mixtures.[27] ^{1}H NMR end-group analysis revealed one-to-one integration of the characteristic protons on either side of the ester linkage, confirming the complete conversion of hydroxyl end-groups to norbornenyl functionalities.

The aPP-NB macromonomers (M_n = 2.05 kg/mol) were then polymerized via ROMP with **G3**. Polymerizations were carried out at room temperature in tetrahydrofuran, and bottlebrushes with various backbone lengths were synthesized by adjusting the feed ratio of catalyst to macromonomer. Products were quenched with an excess of ethyl vinyl ether and isolated by precipitation in methanol. The results are shown in Table 1, and size-exclusion chromatography (SEC) traces of each sample are displayed in Figure 1. Most reactions progressed in a very controlled fashion, indicative of a living polymerization.[28] With the exception of the highest molar mass sample, all polymerizations were complete in less than 10 minutes and resulted in products with low molar mass dispersities ($Đ \leq 1.12$). When targeting higher molar masses, the polymerization rate slowed, and dispersity increased. This is evident in the poly(aPP-NB)_732 sample, which required a 4 hour reaction time and exhibits the largest $Đ$. It is noteworthy

Table 1. Properties of Linear and Bottlebrush Atactic Polypropylene Samples

sample	M_w (kg/mol)[a]	$Đ$[a]	DP[b]	T_g (°C)[c]
aPP-NB	3.38	1.65	-	−25.7
poly(aPP-NB)_11	22.5	1.07	11	−10.0
poly(aPP-NB)_26	53.1	1.03	26	−9.5
poly(aPP-NB)_74	152	1.03	74	−9.0
poly(aPP-NB)_215	440	1.12	215	−9.2
poly(aPP-NB)_732	1500	1.69	732	−9.5
aPP_Linear	203	1.57	-	−7.0

[a]Determined by SEC-MALLS in tetrahydrofuran. [b]Weight-average degree of polymerization of the poly(norbornene) backbone using M_{branch} = 2.05 kg/mol. [c]Glass transition temperature midpoint value measured by DSC.

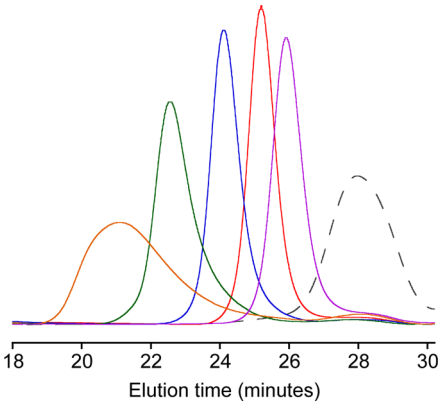

Figure 1. SEC traces (RI signal) of aPP-NB and poly(aPP-NB) samples. Curves correspond to aPP-NB (dashed), poly(aPP-NB)_11 (purple), poly(aPP-NB)_26 (red), poly(aPP-NB)_74 (blue), poly(aPP-NB)_215 (green), and poly(aPP-NB)_732 (orange) and are normalized to the constant integrated area. SEC trace for aPP_Linear is shown in Figure S5 (Supporting Information).

that the SEC traces of each bottlebrush product exhibit a low intensity peak at high elution time. This corresponds to ∼3 wt % nonfunctionalized aPP from the starting material. The final sample listed in Table 1 is a traditional aPP with linear chain architecture that serves as a useful comparison with the bottlebrush polymers.

The linear viscoelastic properties of each polymer were examined by small-amplitude oscillatory shear measurements at temperatures ranging from −20 to 40 °C. Time–temperature superposition of frequency sweep data taken at different temperatures yielded dynamic moduli master curves for each sample. We focus here on dynamic viscosities and the intriguing relationship between zero-shear viscosity and molecular weight for bottlebrush polymers with constant side chain length.

Figure 2 displays the complex viscosity as a function of reduced frequency for aPP-NB and poly(aPP-NB) polymers. To account for differences in glass transition temperatures (T_g) between samples, viscosity data were normalized to a reference temperature of $T_{ref} = T_g + 34$ °C. This reflects room-temperature data for poly(aPP-NB) samples, which all exhibit $T_g \approx -9.5$ °C (see Supporting Information for DSC thermograms). Figure 2 demonstrates that the complex viscosity curves superpose prior to their respective terminal flow regimes. This validates the chosen T_{ref} as an appropriate reference for comparing viscosity data between samples.

dx.doi.org/10.1021/mz500082h | ACS Macro Lett. 2014, 3, 423–427

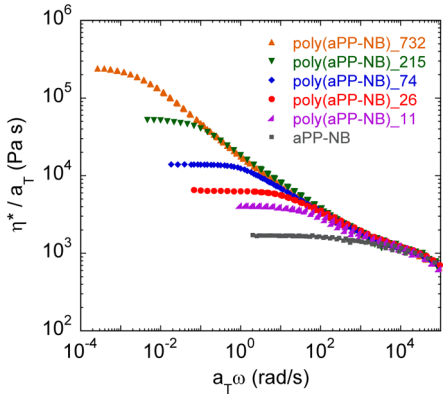

Figure 2. Reduced complex viscosity versus reduced frequency master curves at $T_{ref} = T_g + 34$ °C. Master curve for aPP_Linear is shown in Figure S6 (Supporting Information).

Zero-shear viscosities of each polymer were determined as the terminal η^* values in Figure 2. Typically, the zero-shear viscosity of a polymer melt follows a power law dependence on molar mass described by $\eta_0 \sim M_w^{\alpha}$. For low molar mass polymers, the viscosity obeys the Rouse model prediction, $\alpha = 1$. However, a sharp increase in the power law exponent occurs above a critical molecular weight (M_c) due to the onset of entanglements. An empirical value of $\alpha = 3.4$ describes the scaling of well-entangled melts above M_c.[29] Figure 3 displays the zero-shear viscosities of each aPP sample plotted as a function of molar mass on double logarithmic axes. For comparison, the traditional scaling relationship of linear aPP was also plotted using a critical molecular weight of $M_c = 8.5$ kg/mol.[30]

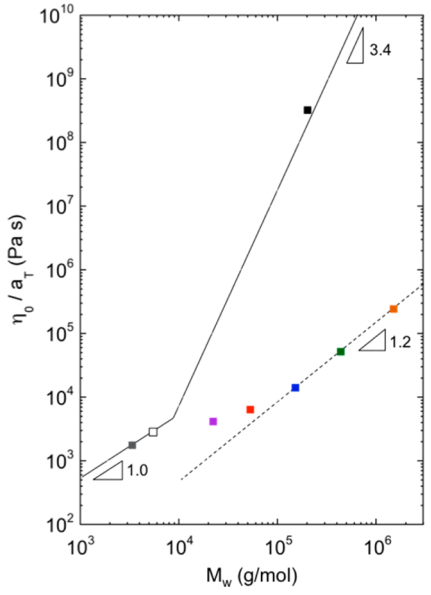

Figure 3. Reduced zero-shear viscosity versus weight-average molecular weight at $T_{ref} = T_g + 34$ °C. The solid line indicates the traditional scaling of linear aPP with a critical molecular weight of $M_c = 8.5$ kg/mol. Data points along this line represent the aPP-NB macromonomer (gray), the aPP_Linear sample (black), and a hypothetical dimer with backbone DP = 2 (open symbol). The remaining solid markers represent poly(aPP-NB) bottlebrush samples listed in Table 1 and fall far below the traditional scaling line. A power-law fit to the highest molar mass data points yields a scaling exponent of $\alpha = 1.2$ (dashed line).

The two data points in Figure 3 at the lowest molar mass represent the aPP-NB macromonomer (gray symbol) and the hypothetical "dimer" with a backbone DP = 2 (open symbol). Since the dimer also represents a linear aPP molecule, it is expected to maintain Rouse dynamics and is plotted along the traditional aPP scaling line. The aPP_Linear sample exhibits a much higher zero-shear viscosity, which is also accordant with the predicted theoretical value. In contrast, the bottlebrush samples show a significant departure from the linear aPP relationship, and two distinct scaling regimes emerge with the addition of more side chains beyond the dimer. The low molar mass region represents a transition zone in which the viscosity dependence on molar mass is extraordinarily low ($\alpha < 0.5$). In the high molar mass region, the scaling is marginally greater than the linear relationship predicted by the Rouse model ($\alpha = 1.2$), suggesting that these polymers remain largely unentangled. Previous studies also have reported unentangled behavior for high molar mass bottlebrush polymers based on the absence of rubbery plateau regions in frequency sweep master curves.[7−13] This is a remarkable consequence of the bottlebrush architecture and has proven particularly beneficial in block copolymer systems for creating ordered morphologies with unprecedentedly large domain sizes.[31−33]

Perhaps the most striking feature of Figure 3 is the weak dependence of viscosity on molar mass in the scaling transition zone, particularly considering Rouse scaling of $\alpha = 1$ signifies the lower limit in traditional polymer melts. This result is fundamentally related to the conformational properties of molecules in this system. Recent investigations have found that a conformational transition occurs in bottlebrush polymers with increasing backbone degree of polymerization (DP). Bottlebrushes with sufficiently short backbones maintain a spherical or globular conformation under good solvent conditions. As the backbone length begins to exceed the length of the brush diameter (D), the molecule transitions to a cylindrical shape that extends one-dimensionally with increased backbone DP. This behavior has been shown in molecular simulations[34] and experimentally by small-angle neutron scattering measurements of bottlebrush polymers in good solvent.[35] The same type of conformational transition is assumed to occur in the melt state as the backbone length is increased. Figure 4 illustrates bottlebrush polymers prepared in this study. The length-to-diameter aspect ratios (L/D) of the bottlebrushes are also given for the four highest molecular weight samples, assuming fully extended chain conformations. An aspect ratio of $L/D = 1$ is calculated to occur at a backbone DP ≈ 38 for this system (see Supporting Information). Thus, the transition from a globular to cylindrical molecular conformation likely occurs between the poly(aPP-NB)_26 and poly(aPP-NB)_74 samples. This is consistent with the observed changeover between scaling regimes in Figure 3 (i.e., where the transition zone ends).

However, the shift in conformation does not directly explain the corresponding viscosity scaling in the two regimes. For instance, linear polymer chains assume a spherical, Gaussian coil conformation in the melt at all molar masses and maintain Rouse-like behavior ($\alpha = 1$) prior to the onset of entanglements. So why is Rouse scaling realized for the large cylindrical bottlebrushes but not for the smaller, more spherical poly(aPP-NB) samples? We posit that this unusual behavior is a result of the space-filling nature of these polymers.

dx.doi.org/10.1021/mz500082h | ACS Macro Lett. 2014, 3, 423−427

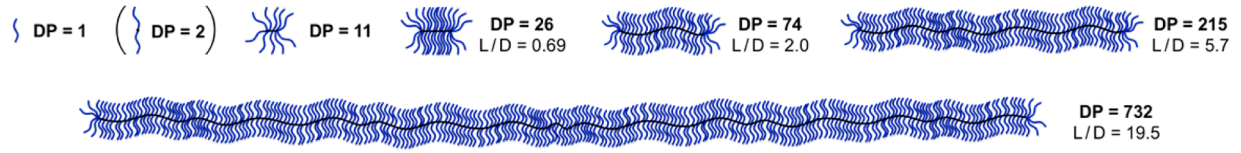

Figure 4. Schematic of the bottlebrush polymers, aPP-NB macromonomer, and hypothetical "dimer" with backbone DP = 2. Length to diameter aspect ratios (L/D) are given for the highest molecular weight bottlebrushes assuming fully extended polymer chains.

As side chains are first added to the growing polymer backbone, each additional arm is forced to occupy the same local space as the previously attached arms. Thus, the continued addition of densely spaced side chains forces the resident arms to compress closer to one another. The increasingly compact molecular structure steadily restricts the number of intermolecular contacts made per repeat unit, particularly near the backbone chain, and reduces the effective friction or drag per monomer segment. Therefore, increasing the molar mass in the form of added side chains will not lend directly to the increased molecular friction, and a sublinear $(\alpha < 1)$ dependence of η_0 on M_w arises. It is not until the backbone is of approximately equal length to the brush diameter that the effective friction per monomeric segment achieves a plateau value. Further attachment of side chains simply causes one-dimensional extension of a cylindrical bottlebrush with constant radial segment density. Since the effective friction per segment is approximately constant, high molecular weight bottlebrush polymers are dynamically similar to unentangled linear polymer coils; i.e., increases in the molecular weight contribute proportionally to the viscosity and result in a near Rouse-like scaling behavior.

In conclusion, a series of bottlebrush polymers with variable backbone length were efficiently synthesized by ROMP of aPP-NB macromonomers using **G3**. A plot of η_0 versus M_w illuminates a scaling transition that is unique to this molecular architecture, i.e., bottlebrush polymers with constant side chain length. Bottlebrush polymers with relatively short backbone chains exhibit remarkably weak dependence of zero-shear viscosity on molar mass, which results from the decreasing net friction per segment as the side chains become more densely packed. At higher backbone DP, bottlebrush polymers undergo a sphere-to-cylinder conformational transition,[35] which is manifested in the Rouse-like scaling of $\alpha = 1.2$ in the high molar mass regime.

■ ASSOCIATED CONTENT

Supporting Information

Experimental details, ^{1}H NMR spectra, DSC thermograms, SEC trace and complex viscosity master curve for the aPP_Linear sample, and additional calculations. This material is available free of charge via the Internet at http://pubs.acs.org.

■ AUTHOR INFORMATION

Corresponding Authors

*E-mail: hillmyer@umn.edu (M.A.H.)
*E-mail: bates001@umn.edu (F.S.B.).

Notes

The authors declare no competing financial interest.

■ ACKNOWLEDGMENTS

ExxonMobil Chemical Company provided the vinyl-terminated atactic polypropylene starting material and financial support for this work. We thank Pat Brant and John Hagadorn for helpful discussions.

■ REFERENCES

(1) Sheiko, S. S.; Sumerlin, B. S.; Matyjaszewski, K. *Prog. Polym. Sci.* **2008**, *33*, 759−785.
(2) Peng, S.; Bhushan, B. *RSC Adv.* **2012**, *2*, 8557.
(3) Zhang, M.; Müller, A. H. E. *J. Polym. Sci. A: Polym. Chem.* **2005**, *43*, 3461−3481.
(4) Wintermantel, M.; Schmidt, M.; Tsukahara, Y.; Kajiwara, K.; Kohjiya, S. *Macromol. Rapid Commun.* **1994**, *15*, 279−284.
(5) Wintermantel, M.; Gerle, M.; Fischer, K.; Schmidt, M.; Wataoka, I.; Urakawa, H.; Kajiwara, K.; Tsukahara, Y. *Macromolecules* **1996**, *29*, 978−983.
(6) Iwawaki, H.; Urakawa, O.; Inoue, T.; Nakamura, Y. *Macromolecules* **2012**, *45*, 4801−4808.
(7) Namba, S.; Tsukahara, Y.; Kaeriyama, K.; Okamoto, K.; Takahashi, M. *Polymer* **2000**, *41*, 5165−5171.
(8) Vlassopoulos, D.; Fytas, G.; Loppinet, B.; Isel, F.; Lutz, P.; Benoit, H. *Macromolecules* **2000**, *33*, 5960−5969.
(9) Tsukahara, Y.; Namba, S.-I.; Iwasa, J.; Nakano, Y.; Kaeriyama, K.; Takahashi, M. *Macromolecules* **2001**, *34*, 2624−2629.
(10) Pakula, T.; Zhang, Y.; Matyjaszewski, K.; Lee, H.-I.; Boerner, H.; Qin, S.; Berry, G. C. *Polymer* **2006**, *47*, 7198−7206.
(11) Hu, M.; Xia, Y.; McKenna, G. B.; Kornfield, J. A.; Grubbs, R. H. *Macromolecules* **2011**, *44*, 6935−6943.
(12) Inoue, T.; Matsuno, K.; Watanabe, H.; Nakamura, Y. *Macromolecules* **2006**, *39*, 7601−7606.
(13) Iwawaki, H.; Inoue, T.; Nakamura, Y. *Macromolecules* **2011**, *44*, 5414−5419.
(14) Lee, S.; Spencer, N. D. *Science* **2008**, *319*, 575−576.
(15) Bolton, J.; Bailey, T. S.; Rzayev, J. *Nano Lett.* **2011**, *11*, 998−1001.
(16) Miyake, G. M.; Piunova, V. A.; Weitekamp, R. A.; Grubbs, R. H. *Angew. Chem., Int. Ed.* **2012**, *51*, 11246−11248.
(17) Miyake, G. M.; Weitekamp, R. A.; Piunova, V. A.; Grubbs, R. H. *J. Am. Chem. Soc.* **2012**, *134*, 14249−14254.
(18) Sveinbjörnsson, B. R.; Weitekamp, R. A.; Miyake, G. M.; Xia, Y.; Atwater, H. A.; Grubbs, R. H. *Proc. Natl. Acad. Sci. U.S.A.* **2012**, *109*, 14332−14336.
(19) Rose, J. M.; Mourey, T. H.; Slater, L. A.; Keresztes, I.; Fetters, L. J.; Coates, G. W. *Macromolecules* **2008**, *41*, 559−567.
(20) Kaneko, H.; Kojoh, S.; Kawahara, N.; Matsuo, S.; Matsugi, T.; Kashiwa, N. *Macromol. Symp.* **2004**, *213*, 335−345.
(21) Anderson-Wile, A. M.; Coates, G. W.; Auriemma, F.; De Rosa, C.; Silvestre, A. *Macromolecules* **2012**, *45*, 7863−7877.
(22) Choi, T.-L.; Grubbs, R. H. *Angew. Chem., Int. Ed.* **2003**, *42*, 1743−1746.
(23) Bielawski, C. W.; Grubbs, R. H. *Prog. Polym. Sci.* **2007**, *32*, 1−29.
(24) Li, Z.; Zhang, K.; Ma, J.; Cheng, C.; Wooley, K. L. *J. Polym. Sci. A: Polym. Chem.* **2009**, *47*, 5557−5563.
(25) Xia, Y.; Kornfield, J. A.; Grubbs, R. H. *Macromolecules* **2009**, *42*, 3761−3766.
(26) Bracher, F.; Litz, T. *J. Prakt. Chem./Chem-Ztg* **1996**, *338*, 386−389.
(27) Jha, S.; Dutta, S.; Bowden, N. B. *Macromolecules* **2004**, *37*, 4365−4374.
(28) Given the dispersity of the aPP-NB macromonomers, it is possible that any size dependence on macromonomer reactivity may lead to a slight gradient in the bottlebrush structure. Any minor gradient nature in the polymers is not expected to impact the reported results.

(29) Berry, G. C.; Fox, T. G. *Adv. Polym. Sci.* **1968**, *5*, 261−357.
(30) Fetters, L. J.; Lohse, D. J.; Colby, R. H. In *Physical Properties of Polymers Handbook*; Mark, J., Ed.; Springer: New York, 2007; pp 447−454.
(31) Runge, M. B.; Bowden, N. B. *J. Am. Chem. Soc.* **2007**, *129*, 10551−10560.
(32) Rzayev, J. *Macromolecules* **2009**, *42*, 2135−2141.
(33) Xia, Y.; Olsen, B. D.; Kornfield, J. A.; Grubbs, R. H. *J. Am. Chem. Soc.* **2009**, *131*, 18525−18532.
(34) Hsu, H.-P.; Paul, W.; Rathgeber, S.; Binder, K. *Macromolecules* **2010**, *43*, 1592−1601.
(35) Pesek, S. L.; Li, X.; Hammouda, B.; Hong, K.; Verduzco, R. *Macromolecules* **2013**, *46*, 6998−7005.

dx.doi.org/10.1021/mz500082h | *ACS Macro Lett.* 2014, 3, 423−427